Journal of Applied Research in Water and Wastewater
E-ISSN: 2476-6283
Journal homepage: https://arww.razi.ac.ir

Simulation of photocatalytic degradation of methylene blue in planar microreactor with integrated ZnO nanowires

Fayazeh Rabanimehr, Mehrdad Farhadian*, Ali Reza Solaimany Nazar, Elham Sadat Behineh

Department of Chemical Engineering, Faculty of Engineering, University of Isfahan, Isfahan, Iran.

GRAPHICAL ABSTRACT

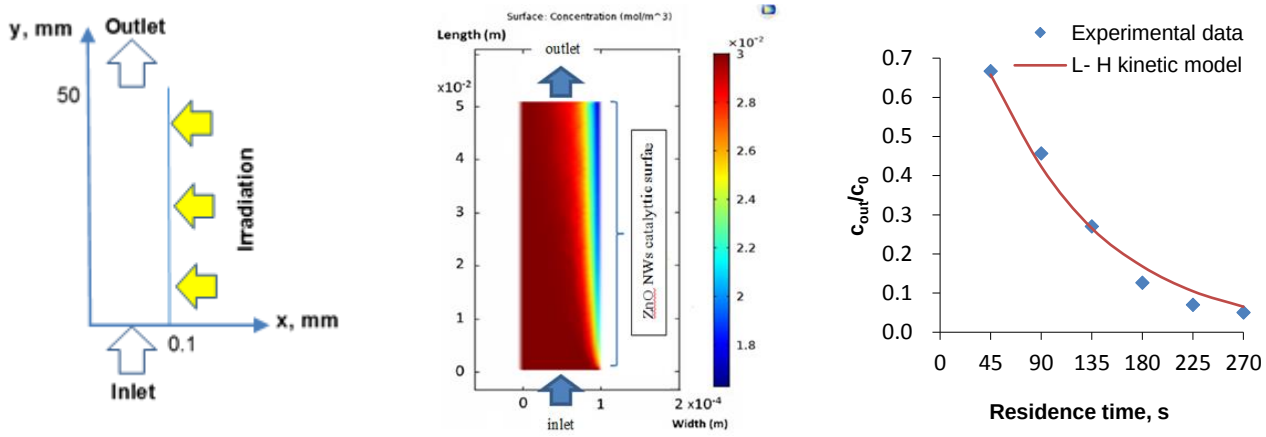

Photocatalytic degradation of methylene blue in planar micro-reactor

ARTICLE INFO

Article history:
Received 6 February 2021
Reviewed 17 April 2021
Received in revised form 27 May 2021
Accepted 29 May 2021
Available online 2 June 2021

Keywords:
Planar microreactor
ZnO nanowires
Simulation
Langmuir–Hinshelwood
COMSOL Multiphysics

Article type: Research Article

Publisher: Razi University

ABSTRACT

In photocatalytic microreactors the catalyst layer is obtained by integration of nanostructure films of semiconductors. One of these nanostructures that have a good photocatalytic activity is ZnO nanowires. The photocatalytic degradation of methylene blue in a continuous flow microreactor with ZnO nanowires deposited film is simulated. A finite element model is developed using COMSOL Multiphysics version 5.3 software to simulate the microreactor performance. The kinetic law of the photocatalytic reaction is assumed to be Langmuir–Hinshelwood. The kinetic constants k_{LHa} and K are determined 1.43×10^{-7} mol/m^{2}s and 7.5 m^3/mol, respectively. The percent of average absolute deviation of the model in predicting the methylene blue outlet concentration obtained about 0.12% mol/m^3. The model showed a very good agreement with the published experimental data. The effect of microreactor depth, methylene blue inlet concentration and flow rate on the methylene blue degradation is also investigated. The simulation results showed that the microreactor with shorter depth and lower values of inlet concentration and flow rate has higher efficiency. Thiele modulus and Damköhler number are both estimated lower than 1. It indicates that the photocatalytic reactions occur without internal and bulk mass transfer limitations.

1. Introduction

Nowadays, due to the increasing demand for clean water, water purification is of particular importance (Wang et al. 2014). However, many contaminants in water and wastewater cannot be treated efficiently by conventional methods (Ali et al. 2016; Jewell et al. 2016; Wang et al. 2016). As a result, the photocatalytic water purification capable of decomposing and mineralizing a wide range of organic pollutants has absorbed attentions (Wa ng et al. 2014). In conventional slurry photoreactors, photocatalysts nanoparticles are homogeneously suspended in an aqueous solution. However, this approach is not efficient due to the non-uniform distribution of light and low photon transfer. Also, recycling the suspended photocatalyst nanoparticles after pollutant removal is a difficult and time consuming process (Dijkstra et al. 2002; Mills et al. 1998). Therefore, it is highly interesting to immobilize the photocatalysts on a solid surface in the form of a film coating. Performing the photocatalytic reactions inside the microreactors with integrated photocatalyst deposited film, has advantages over than in large-size reactors. Short molecular diffusion distance, high surface to volume ratio, fast mixing and high illumination homogeneity are some of the many features of these types of reactors (Wang et al. 2014). Regarding these advantages, integration of nanoporous films of semiconductors like TiO_2 (Krivec et al. 2013) and ZnO (Zhang et al. 2013) into photocatalytic microreactors has been absorbed considerable attentions for organic pollutants removal from water.

*Corresponding author Email: m.farhadian@eng.ui.ac.ir

How to cite: F. Rabanimehr, M. Farhadian, A. R. Solaimany Nazar, E. S. Behineh, Simulation of photocatalytic degradation of methylene blue in planar microreactor with integrated ZnO nanowires, *Journal of Applied Research in Water and Wastewater*, 8 (1), 2021, 36-40.

Charles et al. (2011) investigated salicylic acid photodegradation reaction in a microchannel reactor with immobilized TiO_2 as photocatalyst. They observed that higher salicylic acid photodegradation efficiency can be achieved in higher incident light intensity and lower pollutant concentration and flow rate. They also determined the kinetic constant of salicylic acid photodegradation reaction. Their observations showed that the reaction rate constant is only dependent on incident light intensity. Corbel et al. (2014) studied mass transfer in microchannel photocatalytic reactor experimentally and numerically. They investigated the salicylic acid removal in the presence of immobilized TiO_2 nanoparticulates as photocatalyst. The results of the numerical simulation showed a very good representation of the experimental data. They also established a correlation for Sherwood number that is reliable for all microchannel geometries. Jayamohan et al. (2015) investigated the performance of a planar microreactor with titanium nanotube array (TNA) and TiO_2 nanoparticulate as photocatalysts for methylene blue (MB) degradation and found that the microreactor with TNA photocatalyst has better performance compared to TiO_2 nanoparticulate. They also simulated the performance of the microreactor and deduced that MB degradation efficiency is not affected by mass transfer limitation. He et al. (2010) demonstrated that ZnO nanowires (NWs) could be grown on the inner wall of capillaries and then coated by TiO_2 nanoparticles. This composited photocatalyst showed a reasonable performance.

Han et al. (2013) applied a planar microreactor operating in a close loop with integrated ZnO NWs over a glass substrate for photodegradation of MB. They found that the optimal photocatalytic conditions of microreactor can be obtained with annealed ZnO NWs subjected to UV irradiation. Because the structure of annealed ZnO NWs has better crystallinity and its surface has lower defects compared to unannealed one. This study showed that the ZnO NWs integrated microreactor exhibits more photodegradation efficiency over using suspended ZnO NWs. As the fabrication of microreactors is costly, difficult and time-consuming process, simulation of the microreactors, can be useful for predicting their performances. However, in spite of many experimental works done on photodegradation of organic pollutants in microreactors, simulation and modeling the performance of these systems remains limited.

The aim of this work is to simulate the performance of the integrated ZnO NWs planar microreactor studied by Han et al. (2013). For this purpose, a computational 2-dimensional (2-D) model is setup using COMSOL Multiphysics version 5.3 software to predict the concentration of MB at the outlet of the microreactor. The catalytic surface of the microreactor is assumed to be flat rather than the nanostructured. The kinetic reaction rate constants are estimated by minimization of an objective function. The objective function is defined on the sum of squares of residual concentrations. Dimensionless numbers and the effect of microreactor geometry, inlet concentration and flow rate on MB degradation efficiency are also investigated.

2. Microreactor specifications

The simulated microreactor is planar with annealed ZnO NWs catalytic surface at the bottom, which is subjected to UV light (365 nm) irradiation. The ZnO NWs have been grown on a glass substrate using hydrothermal method and the microreactor has been made from polydimethylsiloxane using soft lithography method. The inner diameter of inlet and outlet tubes of the microreactor is 0.89 mm. Fig. 1 shows the 3-D geometry of the investigated microreactor. Table 1 shows the microreactor geometric specifications. This microreactor is operated in a closed loop and MB solution enters with a fixed flow rate of 400 µl/min. According to the results, the microreactor volume is 75 mm^3 and the residence time of MB solution in the microreactor is 11.25 s in each cycle. The microreactor totally operates in 24 cycles and the MB concentration at the outlet of the microreactor was measured every 4 cycles (Han et al. 2013).

2.1. Numerical modeling

The photodegradation of MB in a 2-D domain has simulated by employing finite element method using COMSOL Multiphysics version 5.3 software. The 2-D model domain of the microreactor is shown in Fig. 2.

2.2. Assumptions

The assumptions made for the model are summarized as follows:
Due to dilution of the solution, the physical properties of water are considered. The steady state condition is considered. It is assumed that the effects of the capillary force are negligible in the microreactor.
It is considered that the photocatalytic degradation of MB takes place on the side covered with photocatalyst film in the microreactor.
It is assumed that the catalytic surface is smooth, unlike it is nanostructured.
The catalytic surface reaction is considered to be equal to the boundary flux at the catalytic surface.

2.3. Model

A single phase, Newtonian and incompressible flow has been considered in the microreactor. The Navier-Stokes and the continuity equations are used for conservation of momentum and mass respectively, to simulate the laminar flow through the microreactor.

$$\rho\left(\frac{\partial \vec{u}}{\partial t}\right)+\vec{u}.\nabla\,\vec{u}=-\nabla\,\vec{p}+\mu\nabla^2\vec{u} \quad (1)$$

$$\rho\nabla\vec{u}=0 \quad (2)$$

where, u is the flow velocity field, ρ is the fluid density, μ is the dynamic viscosity of the fluid and p is the fluid pressure. ρ = 1000 kg/m^3 and μ = 0.001 Pas are used in calculations. The boundary conditions are imposed as follows: at the inlet of the microreactor, the inlet mass flow rate is known so the inlet velocity is uniform in y direcrion and no-slip boundary condition is considered at the channel surfaces. Also, the relative fluid pressure at the outlet of the microreactor is zero.

A convection-diffusion equation is adopted to describe the species mass transfer in the bulk of the microreactor:

$$\frac{\partial \vec{c}}{\partial t}=-\nabla.(-D\nabla\vec{c}+\vec{c}\vec{u}) \quad (3)$$

where, c is the concentration of species and D is diffusion coefficient of the species. In Eq. 3, steady-state condition is considered. The concentration of MB at the inlet of the microreactor is known and the MB concentration gradient at the outlet of the microreactor is equal to zero. At the reactor walls insulating condition is considered. The degradation reaction of MB is done at the ZnO NWs catalytic surface of the microreactor. The photocatalyst absorbs a photon with energy equal to or exceeded than its band gap energy and produces the electron and hole in its conduction and valence bands, respectively. The photogenerated holes oxidize water and produce hydroxyl radicals. Also, electrons produce the superoxide radicals by reduction of dissolved oxygen. The generated free radicals degrade most organic water pollutants like MB at the surface of the photocatalyst. As mentioned in assumptions, the catalytic surface reaction r_a (mol/m^2s) is considered to be equal to the boundary flux at the catalytic surface:

$$r_a=-D\nabla c_s \quad (4)$$

where, c_s is surface concentration of MB. The rate of removal of MB is described by Langmuir–Hinshelwood (L-H) kinetic model which is an adsorption-kinetic model and is applicable for photocatalytic removal of organic pollutants from water (Corbel et al. 2014):

$$r_a=\frac{k_{LHa}\,K\,c_s}{1+K\,c_s} \quad (5)$$

where, K is adsorption constant in m^3/mol and k_{LHa} is the surface reaction rate constant in mol/m^2s, which is calculated from k_{LH}/κ, where k_{LH} is the volumetric reaction rate constant in mol/m^3s and κ is the specific surface area in 1/m. To predict the average MB concentration at the outlet of the microreactor, the Langmuir–Hinshelwood kinetic constants (k_{LHa} and K) must be determined previously. For determination of these parameters, an objective function is defined as:

$$O.F.=\frac{1}{n}\sum_{i=1}^{n}\left(\frac{c_i^{calc.}-c_i^{exp.}}{c_i^{exp.}}\right)^2 \quad (6)$$

where, $c_i^{calc.}$ and $c_i^{exp.}$ are calculated and experimental MB concentration at the outlet of the microreactor at each residence time, respectively and n is the number of experimental data points. For determination of k_{LHa} and K, an initial guess was considered for each of them and the objective function was calculated, then the value of parameters was modified several times in a way that the objective function reached its minimum value. The final values of k_{LHa} and K determined 1.43×10^{-7} mol/m^2.s and 7.5 m^3/mol, respectively. For a complete triangular mesh, the extremely fine mesh size was chosen.

3. Results and discussion

3.1. Validation of proposed model

At the given microreactor geometry, the average outlet concentration of MB (C_{out}) was predicted for each residence times. The

MB inlet concentration (C_0) of 0.03 mol/m^3 (Han et al. 2013), the diffusion coefficient of 1.6 × 10^{-10} m^2/s (Jayamohan et al. 2015) and the determined kinetic rate constants are considered. Fig. 3 shows the predicted and experimental concentration of MB at the outlet of the microreactor as a function of residence time. As shown in this figure, there is a very good agreement between experimental data and model results. The percent of average absolute deviation (AAD, %) of the model in predicting the experimental data is determined 0.12 % mol/m^3 using Eq. 7:

$$AAD=\frac{1}{n}\sum_{i=1}^{n}\left|c_i^{calc.}-c_i^{exp.}\right| \quad (7)$$

As illustrated in Fig. 3, the deviation between the model results and the experimental data points is low at all residence times. As expected, C_{out} decreases with increasing the residence time and it corresponds to the longer contact time of MB in the photocatalytic microreactor.

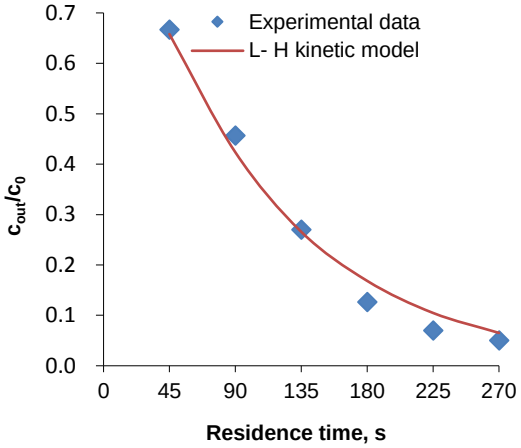

Fig. 3. The model results and experimental data (Han et al. 2013) on MB concentration at the outlet of the microreactor as a function of residence time, C_0=0.03 mol/m^3 and flow rate= 400 µl/min.

3.2. Velocity distribution

Fig. 4 shows the velocity profile in the microreactor. As shown in this figure, the flow regime is laminar. The velocity component perpendicular to the photocatalytic surface is assumed to be zero and the velocity profile parallel to the photocatalytic surface, follows a Gaussian distribution.

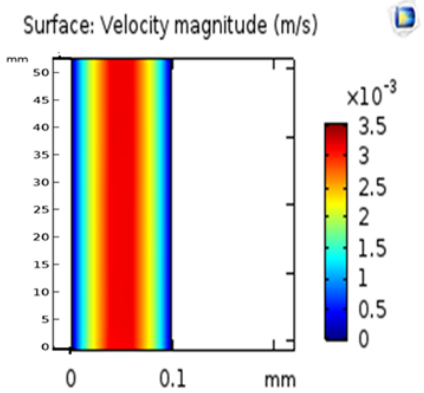

Fig. 4. Velocity distribution in the 2-D domain of microreactor, residence time=11.25 s, C_0=0.03 mol/m^3 and flow rate= 400 µl/min. (For clarity reason dimensions are not real).

3.3. Concentration distribution

Fig. 5 shows the concentration distribution of MB in the 2-D domain of the microreactor at residence time equal to 11.25 s (first cycle). The molecular diffusion of MB from the bulk towards the catalytic surface of ZnO NWs can be seen in this figure. As the photocatalytic degradation reaction happens at the catalytic surface, the MB concentration reduces at the bottom wall of the microreactor. The average outlet concentration of MB at this low residence time is about 0.027 mol/m^3. In this residence time, a concentration gradient is formed in the x-direction, hence the reactant molecules diffuse to the catalytic film, but the residence time is not enough to allow the conversion of all the reactant molecules.

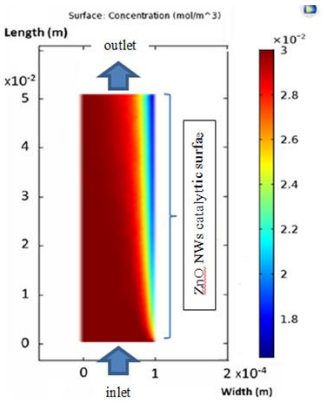

Fig. 5. Concentration distribution of MB in the 2-D domain of microreactor, residence time=11.25 s, C_0=0.03 mol/m^3 and flow rate= 400 µl/min (For clarity reason dimensions are not real).

3.4. Characteristic times

For further scaling analysis on the investigated microreactor, the characteristic times are estimated and summarized in Table 2.

Table 2. Characteristic times.

Parameter	Symbol	Definition	Values
Residence time	t_R	V_R/Q	45-270 s
Diffusion time (in the fluid)	t_D	h^2/D	62.5 s
Effective diffusion time (in the ZnO NWs)	t_{De}	h_0^2/D_e	5.5 s
Reaction time	t_k	$1/k_{app}$	90.9 s

The residence time, $t_R=V_R/Q$, shows the advective transport of MB molecules by the fluid flow parallel to the surface immobilized by ZnO NWs, where V_R is the reaction volume and Q is the flow rate. The diffusion time $t_D = h^2/D$, shows the time required for molecular diffusion of MB in x direction, where h is the depth of microreactor and D is the molecular diffusion coefficient. To intend the diffusion inside the porous ZnO NWs catalyst layer, the effective diffusion time $t_{De} = h_0^2/D_e$ is employed, where $D_e = D\varepsilon/\tau$ is the effective diffusion coefficient, ε is the porosity, and τ is the tortuosity of the photocatalyst film which considering ε = 0.45 and τ = 1.0. The characteristic reaction time can be defined as the reciprocal of the kinetic rate constant: $t_k = 1/k_{app}$. As mentioned in section 3, the values of k_{LHa} and K are 1.43×10^{-7} mol/m^2.s and 7.5 m^3/mol, respectively and k_{app} defined as $k_{app}= k_{LHa}\times K\times \kappa$.

As shown in Table 2, the value of reaction time is more than both the values of diffusion time and effective diffusion time, so it can be concluded that this microreactor is reaction limited and the diffusion of MB molecules in the bulk of fluid and solid is done faster than the reaction. Also, to investigate the mass transfer resistance within the catalyst film, Thiele modulus has been calculated. Thiele modulus $\phi = (t_{De}/t_k)^{0.5}$ represents the ratio of internal diffusion to kinetic time (Aillet et al. 2015, Yusuf et al. 2019) and is estimated to be 0.24 that is lower than 1. So it can be assumed that the reaction occurs in the catalytic film without internal mass transfer limitations.

3.5. Parametric study

3.5.1. Effect of microreactor depth on MB degradation

As shown in Table 1, the depth of the microreactor is very low (h=0.1 mm) and its specific surface area has a higher value (κ=10 1/mm^{-1}) compared to conventional reactors. To investigate the effect of microreactor depth on MB degradation, the performance of the same microreactor with different values of depth is simulated using COMSOL Multiphysics software. The degradation of MB is defined as:

$$X=\frac{C_0-C_{out}}{C_0} \quad (8)$$

where, X is the mean conversion ratio. By increasing the depth of microreactor, the residence time of MB solution in the reactor will be increase. The effect of microreactor depth on the MB degradation in constant flow rate is illustrated in Fig. 6. As shown in the figure, increasing the depth of the microreactor leads to decreasing the MB degradation. This can be explained by a lower mass transfer limitation in microreactor with lower depth. To confirm this aspect, the average mass transfer coefficients in microreactors with the depth of 0.1 and 0.2 mm are calculated using simulation results.

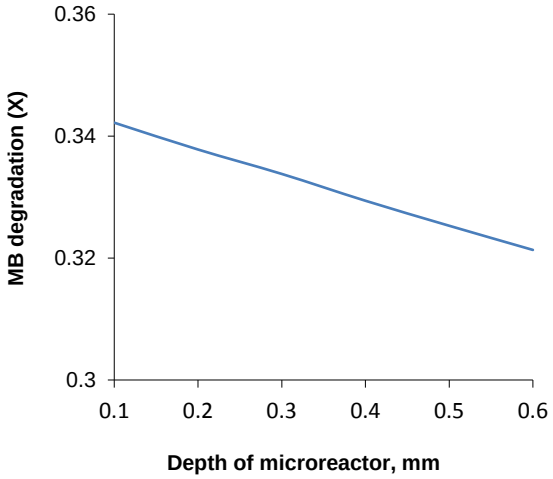

Fig. 6. Effect of microreactor depth on MB degradation, C_0=0.03 mol/m^3 and flow rate= 400 µl/min.

The MB mass flux toward the photocatalytic surface is equal to the rate of reaction. Therefore, the mass transfer coefficient in a horizontal cross section of the microreactor can be calculated using Eq. (9):

$$r_a = k_m(\bar{c}_{MB} - c_{MB_s}) \quad (9)$$

where, k_m is mass transfer coefficient in a horizontal cross section of the microreactor, $\bar{c}_{MB}$ is the average MB concentration in a horizontal cross section of the microreactor and c_{MB_s} is the MB concentration at the catalytic surface of the microreactor. The average mass transfer coefficient $\bar{k}_m$ is considered to be the arithmetical average of mass transfer coefficients at different horizontal cross sections of the microreactor.

For microreactor with depth of 0.1 mm and flow rate of 400 µl/min, $\bar{k}_m$ is determined 1.36×10^{-5} m/s and when the depth of microreactor is 0.2 mm at the same flow rate it is determined 7.5×10^{-6} m/s. Therefore, it can be deduced that increasing the depth of microreactor leads to decreasing mass transfer coefficient and decreases MB degradation. To investigate the effect of mass transfer limitation on the kinetic of MB removal, Damköhler number is calculated. Damköhler number determines that the kinetic of reaction is mass transfer limited or not and is the ratio of the heterogeneous reaction rate at the microreactor wall to radial diffusion of reactant molecules from bulk towards the wall. For photocatalytic reactions that obey the Langmuir–Hinshelwood kinetics, Damköhler number, α is defined as:

$$\alpha = \frac{k_{LHa}}{\frac{k_m}{K} + \frac{k_m}{c_0}} \quad (10)$$

For α less than 0.1, reaction is not mass transfer limited (Charls et al. 2011). The calculated α for microreactor with the depth of 0.1 and 0.2 mm are 0.117 and 0.64, respectively. It can be deduced that microreactor with the depth of 0.1 mm is not mass transfer limited and with increasing the depth to 0.2 mm the mass transfer limitation comes in to existence. Hence, in the microreactor with the depth of 0.1 mm, the intrinsic kinetics can be extracted without computing the mass transfer effects.

3.5.2. Effect of MB inlet concentration on MB degradation

The effect of MB concentration at the inlet of the microreactor on the degradation is investigated at different residence times. As illustrated in Fig. 7, in lower amounts of initial concentration, the microreactor has better efficiency. Because in lower amounts of inlet concentration, there are more active sites of photocatalyst in contact with MB molecules. As shown in the figure, with increasing the residence time, due to the occupation of active sites by MB molecules, the changes in MB degradation decreases and the curves become plateau.

3.5.3. Effect of flow rate on MB degradation

Fig. 8 illustrates the effect of flow rate on the MB degradation in four cycles. As shown in the figure, the microreactor with the lowest flow rate has the highest value of MB degradation. This corresponds to longer residence time of MB solution at lower flow rates.

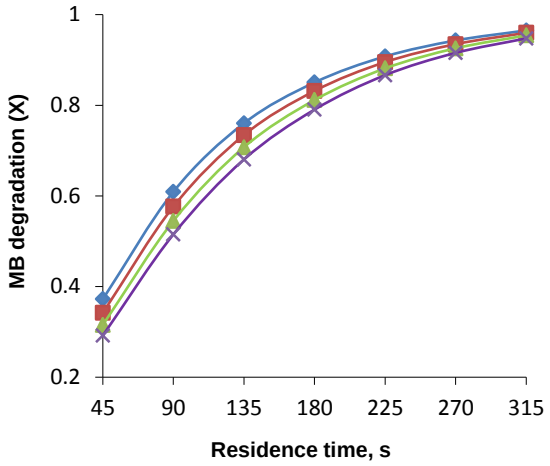

Fig. 7. Effect of MB inlet concentration on MB degradation at different residence times, ♦ symbol shows C_0=0.01 mol/m^3, ■ symbol shows C_0=0.03 mol/m^3, ▲ symbol shows C_0=0.05 mol/m^3 and × symbol shows C_0=0.07 mol/m^3.

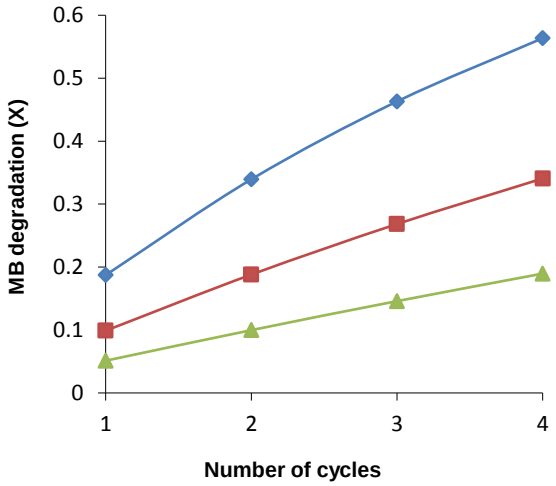

Fig. 8. Effect of flow rate on MB degradation, C_0=0.03 mol/m^3, ♦ symbol shows flow rate= 200 µl/min, ■ symbol shows flow rate= 400 µl/min, ▲ symbol shows flow rate= 800 µl/min.

4. Conclusions

A finite element model was developed using COMSOL Multiphysics 5.3 software to simulate photodegradation of MB in a planar microreactor with integrated ZnO NWs as photocatalyst. The Langmuir–Hinshelwood kinetic constants k_{LHa} and K determined as 1.43×10^{-7} mol/m^2.s and 7.5 m^3/mol, respectively. The model predicted the average concentration of MB at the outlet of the microreactor and showed a very good representation of published experimental data. The percent of average absolute deviation of the model in predicting the experimental data was about 0.12% mol/m^3 and the deviation between the model and the experimental data points was low at all residence times. The simulation results showed that increasing the residence time causes decreasing the MB concentration at the outlet of the microreactor that corresponds to the longer contact time of MB with photocatalyst. The photocatalytic degradation of MB was simulated in different microreactor geometric configurations and it was found that at constant residence time, microreactor with shallower depth has better photocatalytic performance because increasing the depth of the microreactor, leads to higher mass transfer limitation. The simulation results showed that the microreactor has the highest efficiency in the lowest amounts of inlet MB concentration and flow rate. Thiele modulus and Damköhler numbers were estimated and showed that the investigated microreactor performance is not mass transfer limited.

References

Aillet T., Loubie`re K., Prat L., Impact of the Diffusion limitation in microphotoreactors, American Institute of Chemical Engineers Journal, 61 (2015) 1284-1299.

Ali I., Al-Othman Z.A., Alwarthan A., Synthesis of composite iron nano adsorbent and removal of ibuprofen drug residue from water, Journal of Molecular Liquids 219 (2016) 858-864.

Charles G., Roques-Carmes T., Becheikh N., Falk L., Commenge J.M., Corbel S., Determination of kinetic constants of a photocatalytic reaction in microchannel reactors in the presence of mass-transfer limitation and axial dispersion, Journal of Photochemistry and Photobiology A: Chemistry 223 (2011) 202-211.

Corbel S., Becheikh N., Roques-Carmes T., Zahraa O., Mass transfer measurements and modeling in a microchannel photocatalytic reactor, Chemical Engineering Research and Design 92 (2014) 657-662.

Dijkstra M.F.J., Panneman H.J., Winkelman J.G.M., Kelly J.J., Beenackers A., Modeling the photocatalytic degradation of formic acid in a reactor with immobilized catalyst, Chemical Engineering Science 57 (2002) 4895-4907.

Gorges R., Meyer S., Kreisel G., Photocatalysis in microreactors, Journal of Photochemistry and Photobiology A: Chemistry 167 (2004) 95-99.

Han Zh., Li J., He W., Li S., Li Zh., Chu J., Chen Y., A microfluidic device with integrated ZnO nanowires for photodegradation studies of methylene blue under different conditions, Microelectronic Engineering 111 (2013) 199-203.

He Z., Li Y., Zhang Q., Wang H., Capillary microchannel based microreactors with highly durable ZnO/TiO_2 nanorod arrays for rapid high efficiency and continues flow photocatalysis, Applied Catalysis B: Environmental 93 (2010) 376-382.

Helen L., Microfluidic reactors for photocatalytic water purification, Lab on a Chip, 14 (2014) 1074-1082.

Jayamohana H., Smith Y.R., Hansen L.C., Mohanty S.K., Gale B.K., Misra M., Anodized titania nanotube array microfluidic device for photocatalytic application: Experiment and simulation, Applied Catalysis B: Environmental 174-175 (2015) 167-175.

Jewell K.S., Falas P., Wick A., Joss A., Ternes T.A., Transformation of diclofenac in hybrid biofilm activated sludge processes, Water Research 105 (2016) 559-567.

Krivec M., Zagar K., Suhadolnik L., eh M., Drazi G., A highly efficient TiO_2-based microreactor for photocatalytic applications, Applied Material Interfaces 5 (2013) 9088-9094.

Kuo T., Lin Ch., Kuo C., Huang M.H., Growth of ultralong ZnO nanowires on silicon substrates by vapor transport and their use as recyclable photocatalysts, Chemistry of Material 19 (2007) 5143-5147.

Lee K.M., Lai C.W., Koh S.N., Juan J.C., Recent developments of zinc oxide based photocatalyst in water treatment technology: A review, Water Research 88 (2016) 428-448.

Lei L., Wang N., Zhang X.M., Tai Q., Tsai D.P., Chan H.L.W., Optofluidic planar reactors for photocatalytic water treatment using solar energy, Biomicrofluidics 4 (2010) 1-12.

Liao W., Wang N., Wang T., Xu J., Han X., Liu Zh., Zhang X., Yu W., Biomimetic microchannels of planar reactors for optimized photocatalytic efficiency of water purification, Biomicrofluidics 10 (2016) 1-8.

Meng Z., and Zhang XQin., A high efficiency microfluidic-based photocatalytic microreactor using electrospun nanofibrous TiO_2 as a photocatalyst, Nanoscale 5 (2013) 4687-4690.

Mills A., and Wang J.S., Photomineralisation of 4-chlorophenol sensitised by TiO_2 thin films, Journal of Photochemistry & Photobiology. A Chemistry118 (1998) 53-63.

Ould-Mame S.M., Zahraa O., Bouchy M., Photocatalytic degradation of salicylic acid on fixed TiO_2- kinetic studies, International Journal of Photoenergy 2 (2000) 59-66.

Ramos B., Ookawara S., Matsushita Y., Yoshikawa S., Low-cost polymeric photocatalytic microreactors: Catalyst deposition and performance for phenol degradation, Journal of Environmental Chemical Engineering 2 (2014) 1487-1494.

Wang Y., Ma J., Zhu J., Ye N., Zhang X., Huang, H., Multi-walled carbon nanotubes with selected properties for dynamic filtration of pharmaceuticals and personal care products, Water Research 92 (2016) 104-112.

Wang N., Zhang X., Chen B., Song W., Chan N.Y., Chan H.L., Microfluidic photo-electrocatalytic reactors for water purification with an integrated visible-light source, Lab on a Chip, 12 (2012) 3983-3990.

Yusuf A., Oladipo H., Yildiz Ozer L., Garlisi C., Loddo V., Abu-Zahra M. R.M., Palmisano G., Modelling of a recirculating photocatalytic microreactor implementing mesoporous N-TiO_2 modified with graphene, Chemical Engineering Journal 391 (2020) 123574-1-33.

Zhang Q., Wang H., Li Y., A high efficiency microreactor with Pt/ZnO nanorod arrays on the inner wall for photodegradation of phenol, Journal of Hazardous Materials 15 (2013) 318-324.